THE JOURNAL OF PHYSICAL CHEMISTRY B

pubs.acs.org/JPCB Article

Comprehensive Characterization of Lipid-Guided G Protein-Coupled Receptor Dimerization

Published as part of The Journal of Physical Chemistry virtual special issue "Computational and Experimental Advances in Biomembranes".

Stefan Gahbauer* and Rainer A. Böckmann*

Cite This: *J. Phys. Chem. B* 2020, 124, 2823–2834 Read Online

ACCESS | Metrics & More | Article Recommendations | Supporting Information

ABSTRACT: Dimerization of G protein-coupled receptors (GPCRs) is considered to take part in regulating the highly dynamic nature of receptor function. Intensive research unraveled a large variety of different dimer configurations with potentially distinct activity profiles. Studies are complicated by the critical role of the membrane environment for receptor dimerization, and experimental deficiencies in modulating the same. Here we chose a molecular dynamics strategy to characterize the potential of the large chemical lipid repertoire to steer dimerization fingerprints of the neurotensin 1 receptor. Unfavorable hydrophobic mismatch results in excessive dimerization whereas particular lipid features, e.g., anionic headgroups, induce specific dimer interfaces via direct protein−lipid interactions. Polyunsaturated fatty acids attenuate compact dimer formation by facilitated adhesion to the protein transmembrane surface, and receptor lipidation-induced conformational changes confer modulated protein−lipid and protein−protein interactions. Our results highlight the striking role of the membrane environment on GPCR dimerization with potential functional consequences.

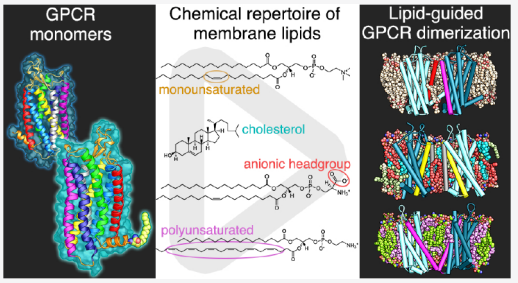

INTRODUCTION

G protein-coupled receptors (GPCRs) form the largest family of transmembrane receptors and are crucial for a wide variety of physiological processes. Their main task is the recognition of extracellular signals, such as small molecules, peptides, or photons, and the induction of intracellular responses via coupling to their eponymous G proteins or interactions with arrestins.[1] Due to their role in many essential signaling pathways and the accessibility of their extracellular ligand binding pocket, GPCRs are the most frequently drug-targeted protein class.[2,3] GPCRs share the general architecture of seven transmembrane helices (TM1 to TM7) and typically show the intracellular helix 8 (H8) perpendicular to the transmembrane helix bundle. As is true of many other membrane proteins, GPCRs interact with their lipid environment. The large chemical reservoir of distinct membrane components offers different mechanisms to regulate protein activity. E.g., membrane nanodomains enriched in either saturated or unsaturated lipids and corresponding differences in bilayer thickness contribute to protein sorting to distinct areas, or specific binding of lipids to protein domains was observed to regulate protein function.[4,5] In the case of GPCRs, membrane properties and specific lipid types were shown to guide localization and allosterically modulate receptor signaling.[6−12] Furthermore, the post-translational addition of the fatty acid palmitate (palmitoylation) to GPCRs was reported as a dynamic process to modulate receptor conformation, localization, activity, and lipid recruitment.[13−17]

For more than 20 years, evidence accumulated that certain GPCRs can form homo- and heterodimers or even higher-order oligomers with potential allosteric functional consequences, e.g., ligand binding cooperativity, modulated intracellular signaling profiles, or altered receptor trafficking.[18−24] In case of class A GPCRs, dimerization and oligomerization were reported to occur as constitutive, transient, and highly dynamic interactions between transmembrane segments.[25−27] Structural information regarding GPCR dimer or oligomer complexes, obtained from, e.g., protein crystallography, Förster or bioluminescence resonance energy transfer (FRET or BRET, respectively), mutagenesis, cross-linking, and computational studies, revealed a variety of different protein−protein interfaces.[28−33] Thus, GPCRs appear able to form multiple dimer interfaces that may exhibit distinct allosteric modulations of receptor activity and function. As the dimerization and oligomerization of class A GPCRs occur mainly between their TM helices, the membrane

Received: January 3, 2020
Revised: March 20, 2020
Published: March 22, 2020

https://dx.doi.org/10.1021/acs.jpcb.0c00062
J. Phys. Chem. B 2020, 124, 2823−2834

Table 1. Summary of Simulation Ensembles[a]

NTS1 dimerization simulation ensemble	membrane	number of simulations	simulation time (μs)	final number of dimers
POPC	100% POPC (C16:0; C18:1)	498	3	264
DEPC	100% DEPC (C22:1; C22:1)	500	3	483
brain polar lipids (BPL)	15% POPC (C16:0; C18:1) 40% POPE (C16:0; C18:1) 20% POPS (C16:0; C18:1) 25% cholesterol	497	8	311
BPL with DHA-containing lipids (BPL-DHA)	15% POPC (C16:0; C18:1) 40% SDPE (C18:0; C22:6) 20% SDPS (C18:0; C22:6) 25% cholesterol	503	8	37
mixture of BPL and BPL-DHA (BPL-DHA-mix)	15% POPC (C16:0; C18:1) 20% POPE (C16:0; C18:1) 20% SDPE (C18:0; C22:6) 10% POPS (C16:0; C18:1) 10% SDPS (C18:0; C22:6) 25% cholesterol	501	8	35
palmitoylated NTS1 (NTS1p) in BPL	15% POPC (C16:0; C18:1) 40% POPE (C16:0; C18:1) 20% POPS (C16:0; C18:1) 25% cholesterol	491	8	174
NTS1p without palmitate in BPL	15% POPC (C16:0; C18:1) 40% POPE (C16:0; C18:1) 20% POPS (C16:0; C18:1) 25% cholesterol	493	8	198

[a]Generated NTS1 dimerization simulation ensembles and used lipid bilayer compositions as well as chemical properties of used fatty acids (number of carbon (C) atoms:number of double bonds) are listed. The number of successfully completed simulations, the length of each simulation, and final numbers of dimers meeting the dimer-acceptance interaction energy criterium (see Supporting Information for details) are shown for all ensembles.

environment was reported to modulate the receptor association;[9] e.g., stabilizing effects of lipids at specific dimer interfaces were suggested for a number of receptors.[34] In particular, computational approaches were employed for in-depth investigations regarding membrane-mediated receptor association.[35−37] Using all-atom (AA) and coarse-grained (CG) molecular dynamics (MD) simulations, specific lipid-binding sites have been identified,[38−43] multiple dimer or oligomeric structures could be explored,[44−47] and the binding affinity between interacting receptors was estimated.[48,49] We previously demonstrated how cholesterol steers chemokine receptor homo- and heterodimerization, possibly inducing the formation of potentially active dimers.[50,51]

The class A GPCR neurotensin receptor 1 (NTS1) and its endogenous peptide ligand neurotensin (NT) are mainly found in cells of the central nervous system and of the gastrointestinal tract, regulating dopamine pathways, hypothermia, muscle relaxation, analgesia, gut motility, and anterior pituitary hormone secretion.[52,53] Pathological processes involving NTS1 and NT are several brain diseases like schizophrenia or Huntington's and Parkinson's diseases, obesity, and various malignancies.[54,55] Different biophysical methods revealed NTS1 receptor dimers *in vitro* and recently *in vivo*.[56−61] Using FRET techniques, NTS1 dimerization was reported as sensitive to the lipid environment[62] and increasing receptor densities resulted in enhanced NTS1 association.[58,59] A recent combination of single-molecule FRET (smFRET) and double electron−electron resonance (DEER) spectroscopy of receptors reconstituted in "native-like" brain polar lipid (BPL) liposomes revealed dynamic association patterns of NTS1 with multiple dimer configurations such as symmetric TM5,6/TM5,6, TM3,4/TM3,4 and TM1,2,H8/TM1,2,H8 interfaces.[59] In addition to dimerization, ligand-binding and G protein-coupling activity of NTS1 were shown to be regulated by the lipid environment.[62−65] E.g., anionic lipids showed increased affinities at the receptor surface compared to neutral lipid types and were suggested to increase NTS1-catalyzed nucleotide exchange at G_q proteins.[63,65] In addition, palmitoylation of NTS1 at cysteine residues on H8 was reported to modulate receptor signaling by guiding the receptor localization within membrane microdomains.[66]

Here, we investigate dimerization patterns of NTS1 receptors in various lipid environments differing in membrane thickness, degree of lipid saturation, or headgroup chemistry and their modulation by receptor palmitoylation. Our strategy of employing ensembles of molecular dynamics simulations for spontaneous receptor self-association permits access to the molecular fingerprints of receptor dimerization and their characteristic modulation by gross membrane properties and by specific protein−lipid interactions. The results presented here for the NTS1 receptor are consistent with available experimental data and highlight the particular importance of membrane nanodomain environments for the structure and function of receptor complexes.

METHODS

Detailed information on the applied methods and simulation analysis are provided in the Supporting Information. Briefly, we simulated dimerization of NTS1 in multiple membrane models to characterize distinct effects of the lipid environment on the association of GPCRs. The used receptor model was prepared based on the crystal structure of rat NTS1 solved by Krumm et

https://dx.doi.org/10.1021/acs.jpcb.0c00062
J. Phys. Chem. B 2020, 124, 2823−2834

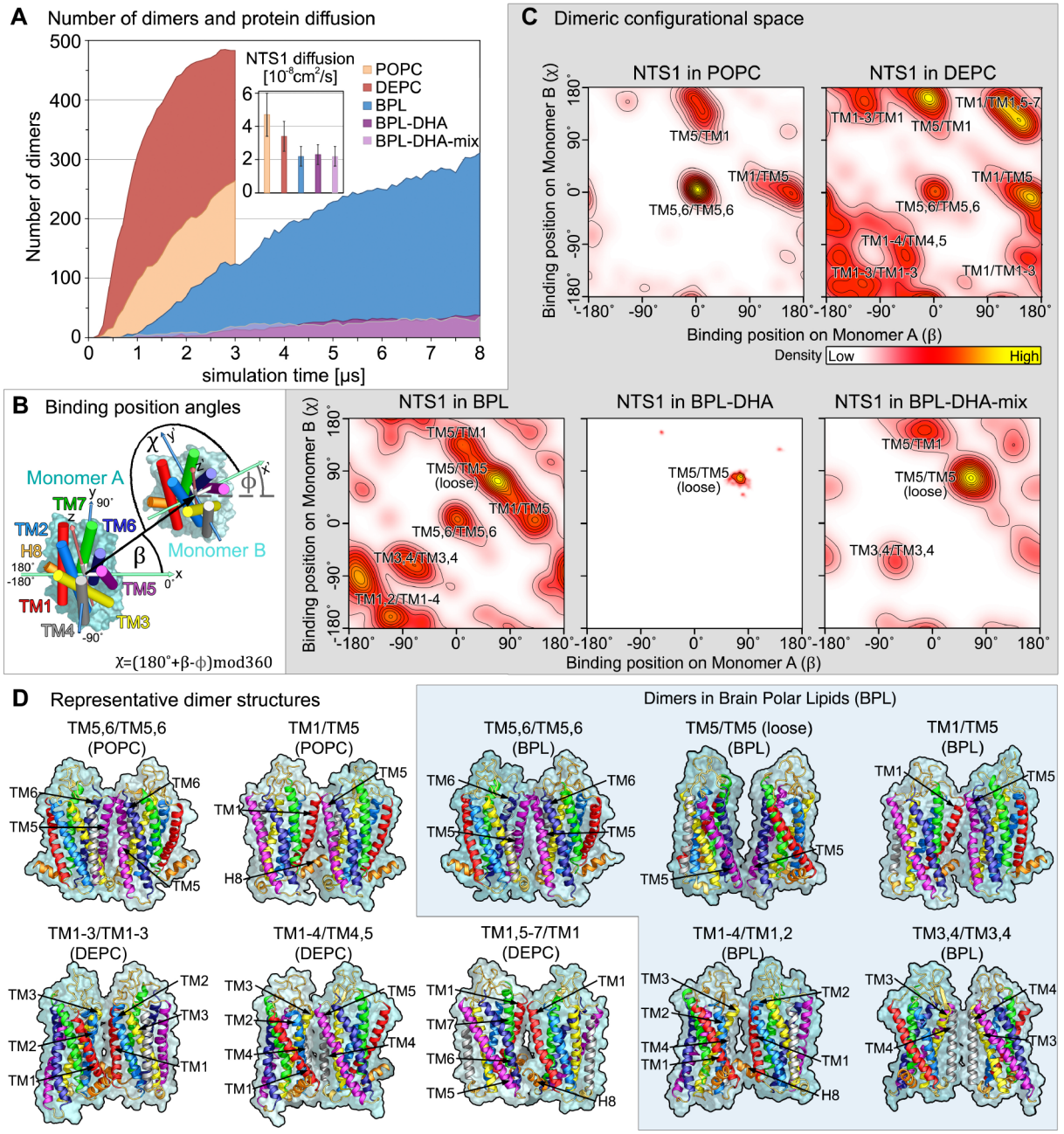

Figure 1. (A) Number of simulations that showed NTS1 dimers according to the dimerization criteria and estimated self-diffusion coefficients (and standard deviations) of monomeric NTS1 in different simulation ensembles (see Supporting Information for details). (B) Orientational analyses for dimer interface determination. The binding position angles β and χ are related to the involved TM helices of monomer A or B at the dimer interface, respectively. (C) Sampled dimer configurations in different simulation ensembles. 2D kernel density estimations for (β,χ)-coordinates were obtained for all dimer structures during the last 50 ns of the simulations. Densities are represented as height-fields with density peaks colored in yellow, followed by moderate densities in red and nonsampled regions in white. (D) Most frequently observed dimer structures of NTS1.

al.[67] and stored in the Protein Data Bank[68] (PDB ID: 4XES). H8 of our NTS1 model was extended by three residues according to the NTS1 crystal structure with PDB ID: 4BUO.[69] Since the third intracellular loop (ICL3) was not resolved in any available structure, ICL3 was simplified by connecting the open ends on TM5 and TM6; i.e., residues V268, P297, G298, R299, and V300 served as an artificial intracellular loop. While we cannot exclude a potential role of ICL3 in NTS1 dimerization, there is only slight evidence indicating an involvement of ICL3 at GPCR dimer interfaces.[70]

A brain polar lipid (BPL) model was based on the commercially available Brain Polar Lipid Extract from Avanti (Catalog No. 141101) assuming a 25% cholesterol content.[65] Seven simulation ensembles, each containing ≈500 independent, microsecond-long simulations of two initially separated NTS1 receptors in defined bilayers were generated following the *DAFT* approach[71] in conjunction with the Martini v2.2 coarse-grained force-field.[72] In individual dimerization simulations, two NTS1 proteins were embedded in roughly 400−500 lipids and each system was simulated for 3−8 μs. Simulation lengths are presented in Table 1. A total MD simulation length of ≈22.8 ms

https://dx.doi.org/10.1021/acs.jpcb.0c00062
J. Phys. Chem. B 2020, 124, 2823−2834

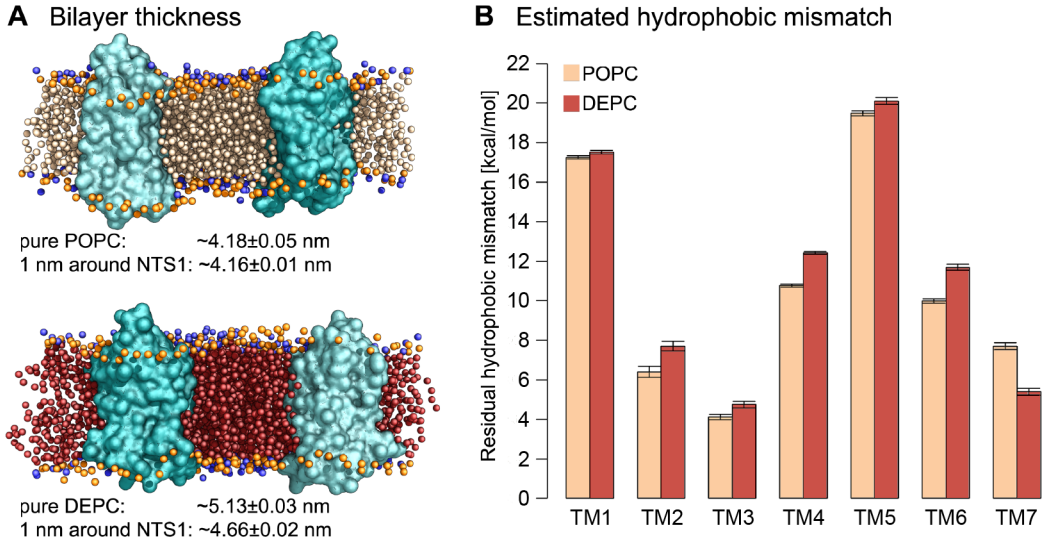

Figure 2. (A) Sample starting structures of two NTS1 proteins in POPC or DEPC. The bilayer thickness was calculated for either protein-free (pure) lipid bilayers or 1 nm around NTS1 receptor monomers. (B) Estimated residual hydrophobic mismatch (and standard errors) of NTS1 in POPC and DEPC bilayers (Mondal et al.;[44] see Supporting Information).

was investigated for NTS1 association patterns. Coarse-grained simulations were performed and analyzed using the GROMACS simulation package version 4.6.[73] The analysis of obtained dimer interfaces followed the protocol previously established by Pluhackova et al.[50] and Gahbauer et al.[51] The residual hydrophobic mismatch was estimated based on the method presented in Mondal et al.[44] Specific protein−lipid interactions and palmitoylation-induced conformational changes were additionally analyzed with atomistic simulations applying the *backward* approach[74] and using the CHARMM36m force field.[75] Receptor monomers were embedded in bilayers containing ca. 600 lipids and MD simulations were performed for 500 ns in case of NTS1 embedded in BPL with 2% SDPE and 2% SDPS lipids, and 1000 ns in case of NTS1 and palmitoylated NTS1 in BPL bilayers with 40% SDPE and 20% SDPS. GROMACS versions 5.1 and 2018 were employed to run and analyze atomistic simulations.[76]

RESULTS AND DISCUSSION

Striving to identify environmental characteristics that potentially modulate GPCR dimerization, we investigated NTS1 receptor association in various lipid environments (see Table 1): in simple 1-palmitoyl-2-oleoyl-*sn*-glycero-3-phoshocholine (POPC) and 1,2-dierucoyl-*sn*-glycero-3-phosphocholine (DEPC) bilayers, as well as in different lipid environments reflecting the main properties and composition of brain polar lipid (BPL) extracts. BPL membranes were frequently used in biophysical studies with reconstituted NTS1.[58,59,62,65] Our BPL model contains lipids with PC, phosphoethanolamine (PE), and anionic phosphoserine (PS) headgroups as well as cholesterol. Since membranes of brain cells were reported to contain increased amounts of stearic and polyunsaturated docosahexaeonic acids (DHA) for PE and PS lipids,[77,78] the influence of 1-stearoyl-2-docosahexaeonly-*sn*-glycero-3-phosphoethanolamine (SDPE) and -phosphoserine (SDPS) lipids was investigated in additional simulation setups. The dimerization of NTS1 was addressed in ensembles containing each ≈500 independent simulations on the microsecond time scale of two randomly rotated, initially separated receptors at a given starting minimum distance (≈3.6 nm).[71,79]

Membrane-Mediated NTS1 Dimerization. Figure 1 summarizes dimerization patterns of NTS1 in the described lipid environments. The final number of dimers (reaching the dimer-acceptance interaction energy criteria, see Supporting Information) and the diffusion coefficient of NTS1 proteins differed drastically between simulation ensembles (see Figure 1A). Although the diffusion of NTS1 in DEPC ($\approx 3.4 \times 10^{-8}$ cm^2/s) was reduced compared to that for POPC ($\approx 4.7 \times 10^{-8}$ cm^2/s), NTS1 dimerization was enhanced by almost a factor of 2 within the DEPC environment on a time scale of 3 μs. This difference in dimerization kinetics thus hints to a substantially different dimerization path. The analysis of dimer interfaces, using relative binding position angles (β, χ) between receptors in dimer complexes (see Figure 1B and Pluhackova et al.[50] for more details), revealed accordingly distinct and composition-dependent association fingerprints for NTS1. Figure 1C shows kernel density estimations for obtained dimer angles, rationalizing the dimer configurational space at the end of each simulation ensemble; representative dimer structures are illustrated in Figure 1D (for a comparison of initial and final NTS1 dimer configurations see Figure S1). In pure POPC membranes, only two distinct dimer interfaces were obtained for NTS1: asymmetric TM1/TM5 and symmetric TM5,6/TM5,6 configurations. In contrast, NTS1 in DEPC bilayers formed a variety of dimers, including additional interfaces involving TM3 and TM4 or symmetric interfaces with TM1. This decreased binding interface specificity within a membrane with a large hydrophobic core thickness caused the increased dimerization rate despite a decreased diffusion.

In a different manner, for a BPL environment, the dimerization rate was lowered with respect to NTS1 dimerization in POPC, similar to the reduction in the receptor diffusion coefficient ($\approx 2.2 \times 10^{-8}$ cm^2/s). In addition to the TM5,6/TM5,6 interface, NTS1 formed largely symmetric interfaces involving TM1,2 or TM3,4. These interfaces are in remarkable agreement with configurations suggested based on DEER experiments conducted in BPL bilayers.[59] Compact dimer formation was severely hampered in BPL bilayers with high amounts of DHA. The few obtained dimers exclusively showed loosely packed TM5/TM5 interactions in the presence

https://dx.doi.org/10.1021/acs.jpcb.0c00062
J. Phys. Chem. B 2020, 124, 2823−2834

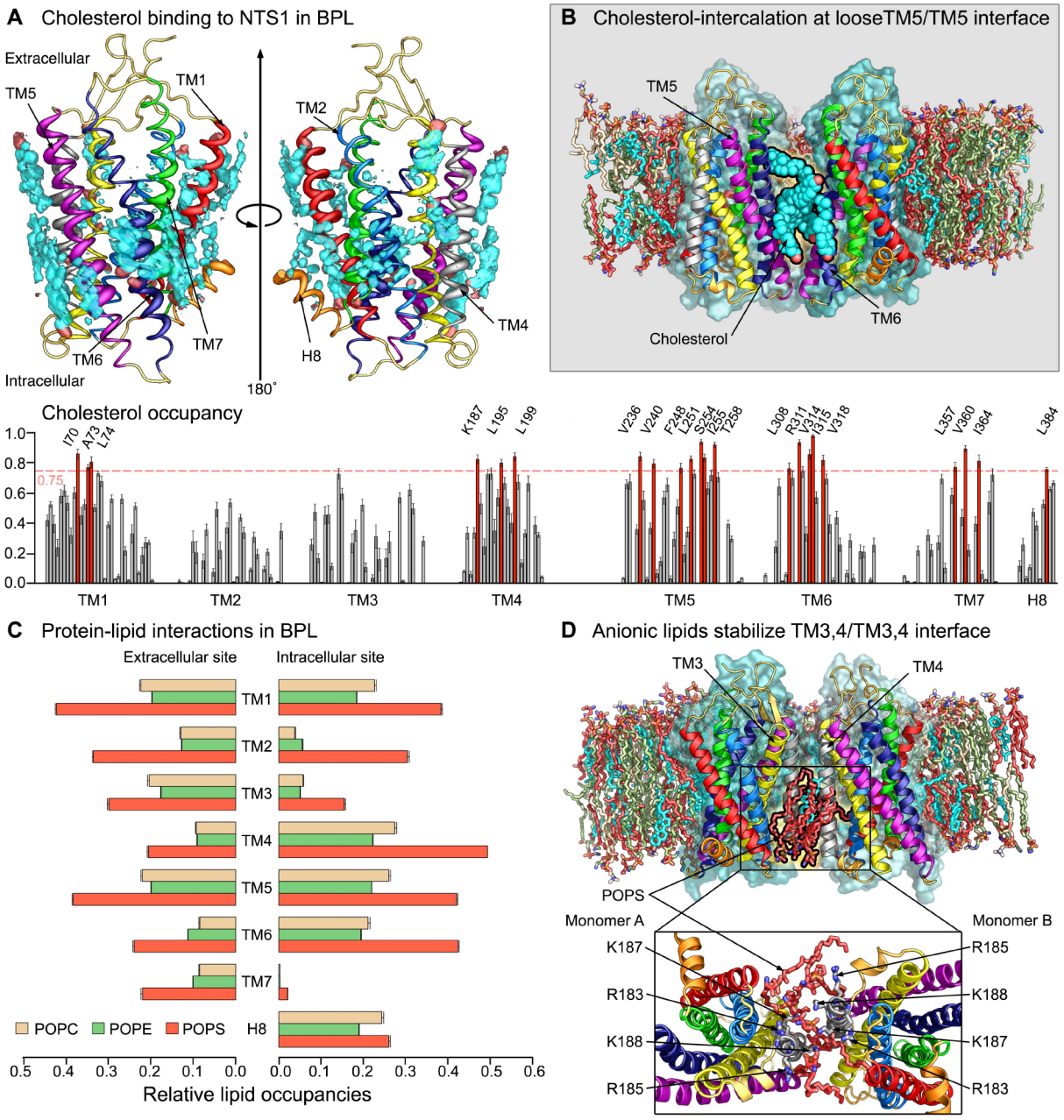

Figure 3. (A) Cholesterol-binding to NTS1 in BPL membranes. The spatial density distribution of cholesterol molecules around NTS1 are shown in cyan, the density distribution of the cholesterol headgroup (ROH) is shown in dark red. The thickness of the cartoon representation of NTS1 corresponds to the cholesterol occupancies of TM residues. The lower panel shows cholesterol occupancies (and standard errors), corresponding to the fraction of simulation time with at least one cholesterol bound to the receptor surface. Highly occupied residues (occupied for more than 75% of simulation time) are highlighted. (B) Cholesterol molecules bound to TM5 and TM6 helices intercalate at the dimer interface in the loose TM5/TM5 configuration. (C) Relative occupancies (and standard errors) of different lipid species at the extracellular and intracellular termini of TM helices and H8. (D) Anionic POPS lipids stabilize the TM3,4/TM3,4 dimer interface by mainly interacting with positively charged, intracellular residues on TM4.

of polyunsaturated lipids (see Figure S2). Interestingly, in mixed bilayers of BPL with reduced concentrations of DHA (BPL-DHA-mix), the small amount of obtained dimers explored a larger configurational space as compared to dimers in BPL-DHA.

These results for NTS1 receptors substantiate the extraordinary impact of membrane compositions on receptor dimerization kinetics and configurations, suggesting mechanisms extending beyond diffusion-limited processes.

Hydrophobic Mismatch Affects Dimer Fingerprints. As shown in Figure 2A, the increased chain length of eruic acid compared to oleic or palmitic acid resulted in DEPC bilayers of ≈5.13 nm thickness, i.e., roughly 1 nm thicker as compared to POPC bilayers (≈4.18 nm). While the thickness of POPC bilayers was hardly influenced by the NTS1 receptor, DEPC bilayers were compressed to a thickness of ≈4.66 nm in the vicinity of NTS1, indicating a significant hydrophobic mismatch between NTS1 and DEPC.

Residual hydrophobic mismatch (RHM) energies for all seven TM helices of NTS1, depicted in Figure 2B, were estimated by penalizing exposed surface areas of hydrophobic residues outside the hydrophobic membrane core and surface

https://dx.doi.org/10.1021/acs.jpcb.0c00062
J. Phys. Chem. B 2020, 124, 2823−2834

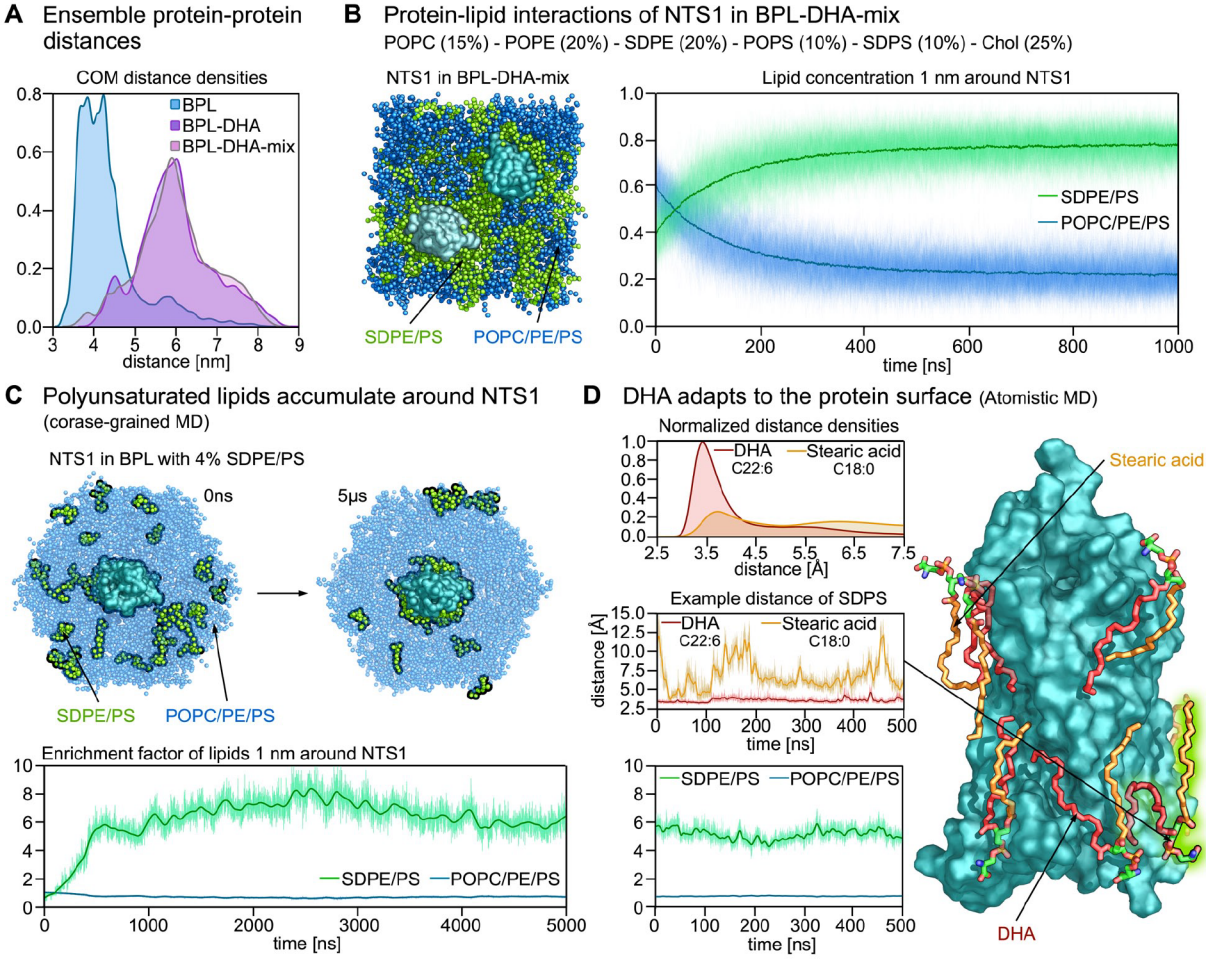

Figure 4. (A) Distribution of transmembrane helix-bundle center of mass (COM) distances during the last 50 ns of simulation time in different ensembles. (B) Interactions of NTS1 with SDPE/PS or POPC/PE/PS lipids. (*Left*) Sample simulation snapshot of two NTS1 proteins in a BPL-DHA-mix bilayer. (*Right*) Average propensities of SDPE/PS or POPC/PE/PS lipids 1 nm around NTS1 receptor monomers in 100 BPL-DHA-mix ensemble simulations during the first microsecond of simulation time. (C) Accumulation of SDPE/PS 1 nm around a NTS1 monomer in a BPL bilayer with 2% SDPE and 2% SDPS. (*Above*) Initial and final snapshots of a 5 μs CG MD simulation. (*Below*) Enrichment factors, i.e., the ratio of the concentration of lipids 1 nm around NTS1 compared to the bulk concentration, plotted against simulation time. (D) Conversion of the final snapshot shown in part C to atomistic resolution and subsequent simulation, confirming the preferred binding of SDPE/PS to NTS1. (*Left*) Distributions of average minimal distances of DHA or stearic acid of bound SDPE/PS lipids and an example of a distance trajectory of a bound SDPS lipid. As in part C, enrichment factors of SDPS/PE and POPC/PE/PS lipids 1 nm around NTS1. (*Right*) Sample snapshot from the atomistic simulation of NTS1 with bound SDPE/PS lipids.

areas of hydrophilic residues within the bilayer core (following the approach presented in Mondal et al.;[44] compare with the Supporting Information). Interestingly, TM1 and TM5 of NTS1 show the highest RHM in POPC bilayers and contribute to all dimer interfaces obtained in the POPC simulation ensemble, indicating a correlation between the hydrophobic mismatch of a transmembrane segment and its involvement at complex interfaces. The total hydrophobic mismatch of NTS1 in POPC ($\approx$ 75.7 kcal/mol) is smaller as compared to that for DEPC bilayers ($\approx$ 79.6 kcal/mol); i.e., the observed increased number of dimers in the DEPC simulation ensemble (see Figure 1A) is likely related to the larger hydrophobic mismatch (see Figure S3 for RHM analysis of other studied membrane compositions). Furthermore, TM2−TM4 and TM6, which contribute substantially to dimer interfaces in DEPC bilayers, show ≈15% increase in RHM. TM7 revealed a reduced RHM in DEPC, however, does typically not contribute to observed dimer interfaces as its surface is structurally masked by TM1 and TM6 and transitions into H8 on the intracellular side.

In brief, longer, mainly saturated fatty acids in DEPC resulted in an elevated hydrophobic mismatch between NTS1 and the membrane environment, resulting in increased dimerization rates and a higher variety of dimer interfaces. Previous experiments indicated pronounced FRET efficiencies between labeled NTS1 reconstituted in POPC in the presence of POPE or cholesterol, i.e., components increasing the bilayer thickness compared to pure POPC bilayers.[62] Our simulation ensemble in DEPC revealed a significantly larger number of possible dimer configurations, allowing to hypothesize that NTS1 in POPC possibly formed less FRET-efficient dimers, while dimers formed in thicker DEPC bilayers, e.g., symmetric interfaces around TM1 or complexes involving TM3,4, may represent FRET-capable configurations.

Specific Lipid Types Stabilize Distinct Dimer Interfaces with Potential Functional Consequences. The BPL model membrane resulted in a bilayer thickness of ≈4.36 nm, with a slightly reduced thickness 1 Å around the embedded NTS1 receptor ($\approx$ 4.24 nm); i.e., the presence of cholesterol and

https://dx.doi.org/10.1021/acs.jpcb.0c00062
J. Phys. Chem. B 2020, 124, 2823−2834

PE lipids increased the bilayer thickness as compared to POPC. As presented in Figure 1C, the dimerization fingerprint of NTS1 in BPL differs significantly from corresponding patterns of NTS1 in POPC or DEPC environments. Specific protein−lipid interactions modulating receptor dimerization are illustrated in Figure 3.

Cholesterol-binding to NTS1 was analyzed by monitoring the cholesterol occupancy at individual TM residues (see Figure 3A). In particular, residues on the intracellular halves on TM5 and TM6 showed elevated cholesterol occupancies. Bound cholesterol molecules could be identified between interacting NTS1 receptors in the loosely packed TM5/TM5 configuration that were only sampled in cholesterol-containing bilayers (see Figure 3B). Cholesterol intercalation stabilizes this noncompact symmetric interface by preventing the extracellular halves on TM5,6 to form tight contacts. Similar to results of previous ESR experiments,[65] pronounced occupancies of negatively charged PS lipids in close vicinity of NTS1 were observed in the simulations (Figure 3C). Particularly the intracellular segment of TM4 preferably bound PS lipid headgroups. Interestingly, the experimentally suggested symmetric TM3,4 dimer interface, only sampled in simulations with BPL membrane models, shows intracellularly intercalating PS lipids between NTS1 in the dimer receptor complex (see Figure 3D). Several anionic lipids could be identified fully pervading the intracellular interface between both receptors, thereby interacting with the enriched positively charged residues on TM4.

Combining previous experimental studies on receptor dimerization and activity of reconstituted receptors at high protein concentration, i.e., with predominately dimeric NTS1 (≈ 90%),[58,59] with the dimer interfaces observed *in silico*, allows for intriguing hypotheses. Compared to NTS1 reconstituted in BPL liposomes, receptors in pure POPC or POPC/cholesterol mixtures revealed reduced dimer FRET efficiencies and a diminished neurotensin-binding activity, indicating the presence of inactive dimer configurations.[62] Our simulation ensembles suggest dimer structures predominately involving TM5,6 in pure POPC or stabilized by cholesterol. I.e., for this dimer conformer, the consensus outward activation-motion of (mainly) TM6 upon ligand-binding[80−82] appears hampered without a change in dimer configuration. Indeed, NT-binding to NTS1 in BPL liposomes was reported to decrease dimer FRET efficiencies between receptors labeled at TM6, indicating changes at the TM5,6 dimer interfaces.[59] Since agonist-binding affinities are significantly increased in fully activated, G protein-coupled states,[83] trapping TM5,6 at the dimer interface may allosterically modulate agonist-binding capabilites of GPCRs by interfering with the transition from inactive to active states.

In turn, the anionic lipid-induced symmetric TM3,4 dimer interface that emerged in simulations using BPL model bilayers (see Figure 3D), presents freely accessible TM5,6 helices. The ligand-induced activation motion and subsequent G protein-coupling appears more likely to occur for receptors in this configuration.[59] In fact, anionic PG lipids were shown to increase nucleotide exchange at G_q proteins coupled to NTS1.[63]

Interestingly, it was suggested that coupling to G_s proteins requires a larger displacement of TM6 as observed in GPCR-G_i complexes.[84,85] Since NTS1 couples promiscuously to all G protein subtypes,[86] dimerization potentially contributes to downstream signaling bias. Indeed, the recently solved cryo-EM structure of NTS1 coupled to G_i allows superposition with NTS1-dimers displaying symmetric TM5,6 interfaces, while structural alignments using the β2 adrenergic receptor-G_s complex results in significant sterical clashes for corresponding interfaces (see Figure S4 for alignments of G protein-bound GPCRs and NTS1 dimer structures). In turn, the TM3,4 dimer interface would allow for G_s and G_i binding.

Polyunsaturated Lipids Accumulate at the Protein Surface and Reduce Compact Dimer Formation. As depicted in Figure 1A, compact NTS1 dimer formation was substantially reduced in DHA-containing bilayers. The center of mass distance distributions between the receptors by the end of all simulations of the respective ensembles, presented in Figure 4A, shows that NTS1 could not form compact dimers in the presence of polyunsaturated lipids, even though the diffusion coefficients remained rather unaffected as compared to BPL bilayers in absence of DHA.

Figure 4B illustrates NTS1-lipid interactions in simulations of BPL mixed with 30% DHA-containing SDPE/PS (BPL-DHA-mix simulation ensemble). As can be seen in a final simulation snapshot, SDPE/PS lipids accumulated around the receptors and formed lipid nanodomains, excluding more saturated POPC/PE/PS lipids. Monitoring the concentration of lipids in a distance of 1 nm around NTS1 in course of the first microsecond of simulations in mixed BPL-DHA bilayers, revealed a rapid increase of DHA-containing lipids in receptor vicinity resulting in stable lipid shells consisting of roughly 20% POPC/PE/PS and 80% SDPE/PS. Similar findings were reported from simulation studies on adenosine and dopamine receptors,[45] and DHA was reported to support GPCR partitioning to ordered membrane domains.[87] Therefore, polyunsaturated fatty acid chains may contribute in sorting GPCRs into distinct membrane nanodomains, thus driving colocalization of GPCRs. To further investigate binding of DHA to NTS1, a protein monomer was embedded in a BPL bilayer containing 2% SDPE and 2% SDPS (see Figure 4C). Simulation snapshots and calculated enrichment factors of lipids in vicinity of NTS1 highlight the accumulation of DHA around the receptor, indicating up to 8-fold higher DHA concentration around NTS1 compared to the bulk composition. Converting the final snapshot of the 5 μs CG simulation to atomistic resolution enabled the detailed investigation of bound SDPE and SDPS lipids (presented in Figure 4D). As illustrated in the protein−lipid structure, flexible DHA is able to penetrate into the rugged protein surface, while fully saturated stearic acids are less tightly bound. Analysis of the distances between fatty acid chains and the protein surface from atomistic simulation revealed a tighter and longer-lasting adhering of DHA as compared to saturated stearic acids.

The preferred binding of DHA to GPCRs was reported before for rhodopsin and simulation studies suggested lower entropic costs for polyunsaturated fatty acids adapting to transmembrane proteins as compared to saturated lipids.[88−90] In combination with the observed depleted formation of compact dimers in DHA-containing simulation ensembles, accumulation of polyunsaturated lipids around NTS1 appears to shield transmembrane segments from engaging in direct protein−protein contacts. Furthermore, the entropically costly adaptation of saturated lipid tails to rugged protein surfaces was suggested as a driving force behind transmembrane protein aggregation (as discussed in, e.g., Sabra et al.[91] or Helms[92]).

Interestingly, Guixà-González et al. reported *enhanced* oligomerization kinetics from coarse-grained simulations and BRET experiments for adenosine and dopamine receptors in DHA-enriched membranes.[45] However, the BRET experiments added DHA and ω-3 fatty acid triglycerides, while SDPC was

https://dx.doi.org/10.1021/acs.jpcb.0c00062
J. Phys. Chem. B 2020, 124, 2823−2834

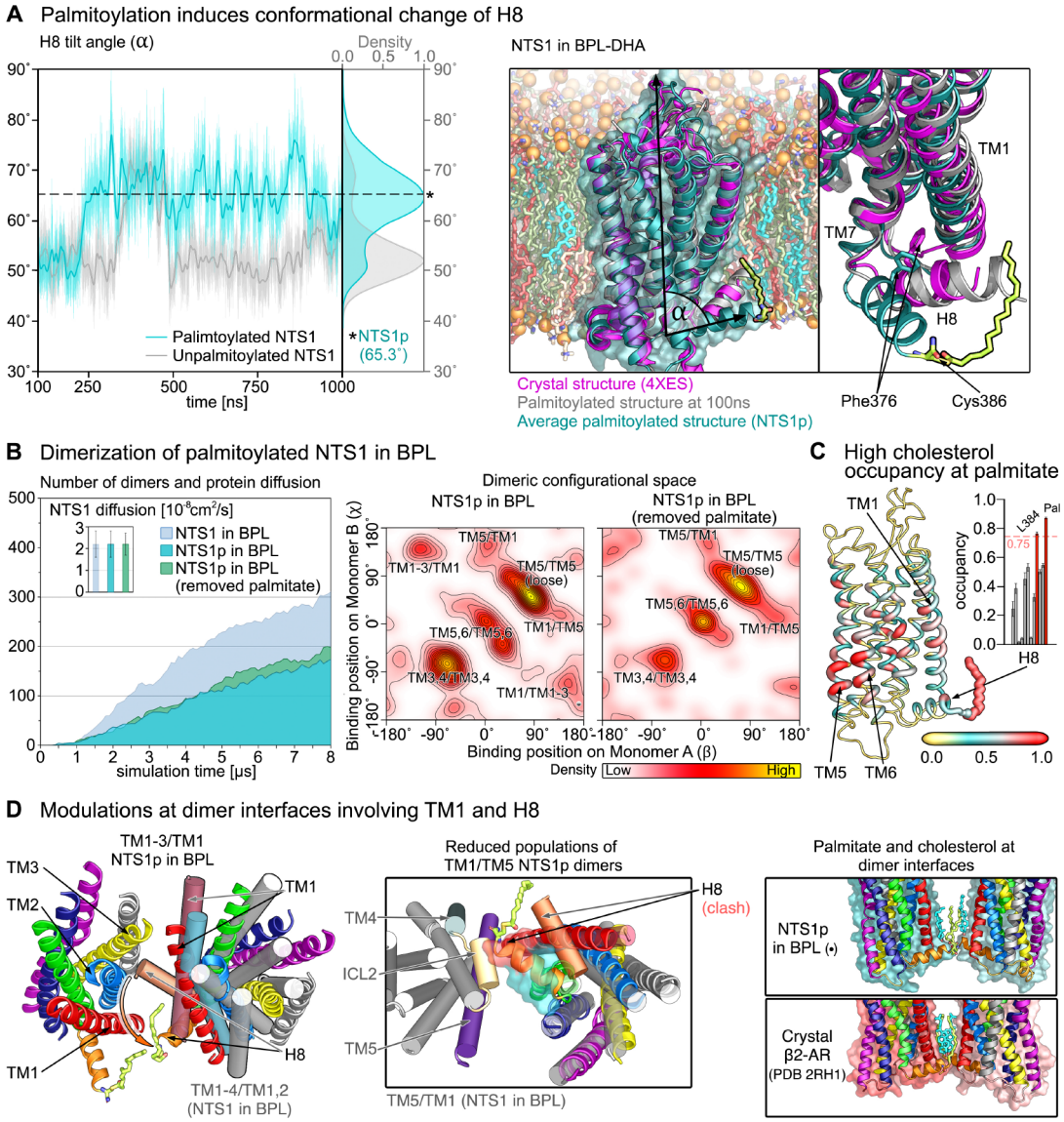

Figure 5. (A) Atomistic simulations of palmitate-free and -anchored NTS1 in BPL-DHA. The tilt angles α between the principal protein axis and the H8 axis were calculated over one microsecond trajectories (first 100 ns neglected for equilibration). The average conformation of the palmitoylated NTS1 receptor (NTS1p) was chosen according to the mean tilt angle during the last 200 ns of the simulation. Phe376, partially inserted into the pocket between TM1 and TM7 in the crystal structure, is no longer anchored in the palmitoylated protein conformation. (B) Dimerization of palmitoylated NTS1 was investigated with simulation ensembles in BPL bilayers. Simulations were computed with either palmitoylated or unpalmitoylated proteins in NTS1p conformation, in order to investigate the impact of the conformational change and the presence of palmitate. (C) Protein helix thickness and color scaled by the cholesterol occupancy of individual residues. (D) NTS1p dimers (helices shown in cartoon representation and colored according to Figure 1B) compared with NTS1 dimers (shown with cylindrical helices and colored in gray with highlighted helices at the dimer interface). As observed in the β2-adrenergic receptor crystal structure,[93] NTS1p was observed to form dimers with cholesterol bound to the palmityl-anchors between receptor monomers (•, position within the configurational space).

used in simulations. In contrast, we added DHA for PE and PS lipids, as suggested in experiments on brain cell membranes.[77,78] Thus, DHA may show different effects on GPCR oligomerization kinetics and patterns, depending both on the type of lipid headgroup and the particular GPCR studied.

Palmitoylation-Induced Modulations of NTS1 Conformation, Dimerization, and Interactions with Cholesterol. Post-translational lipidation of GPCRs presents another important sort of protein−lipid interaction reported to modulate receptor activity and dimerization. In order to investigate palmitoylation of NTS1, microsecond atomistic simulations were carried out for palmitate-free and lipidated receptors carrying a palmitoyl anchor at Cys386 in DHA-containing BPL bilayers. In Figure 5A, the tilt angle α between the first principal axes of H8 and the transmembrane helix bundle indicates a significant conformational change of the palmitoylated H8. Thereby, the palmitoylated H8 adopted a conformation more parallel to the membrane surface and embedded within the membrane interface, while the non-lipidated H8 stayed in a more tilted conformation as observed in the crystal structure ($\approx 52°$). The average conformation of the lipidated H8 during the last 200 ns of simulation was selected as a representative structure for the palmitoylated receptor (we will refer to the palmitoylation-induced receptor conformation as NTS1p). Subsequently, NTS1p was converted to the coarse-

https://dx.doi.org/10.1021/acs.jpcb.0c00062
J. Phys. Chem. B 2020, 124, 2823−2834

grained representation to investigate dimerization of palmitoylated receptors in BPL bilayers.

Dimerization simulation ensembles were conducted for NTS1p carrying the palmitoyl anchor and for receptors in the NTS1p conformation with removed palmitate in order to identify differences caused by the conformational change of H8 only and by presence of the attached fatty acid. Compared to unpalmitoylated NTS1 in BPL, both NTS1p models (i.e., with and without palmitate) showed similar diffusion coefficients, however, a moderately reduced number of dimers after 8 μs of simulation time. The dimer configurational spaces of receptors in NTS1p conformational states revealed decreased numbers of compact interfaces involving TM1 as compared to unpalmitoylated NTS1 (compare Figure 1C), while symmetric TM3,4 and TM5,6 interfaces appeared unaffected by palmitoylation. As illustrated in Figure 5D, the NTS1 TM1,2/TM1−4 dimer interface was reduced and shifted toward TM1−3/TM1 interactions in case of NTS1p. While TM1 and H8 in the crystal-like conformation interacted with TM4 of the dimerization partner in case of TM1,2/TM1−4 complexes, H8 in the corresponding TM1−3/TM1 NTS1p receptor dimer faces TM1 of the adjacent receptor. Furthermore, the palmitoylation-induced conformation of NTS1p-H8 hindered the formation of TM1/TM5 dimers as observed for nonlipidated NTS1, since H8 would clash with residues on the second intracellular loop (ICL2). Pronounced cholesterol binding was observed for the palmitate offering an additional binding spot on H8 (see Figure 5C). Interestingly, a small number of dimer interactions involving the palmitoyl anchors and bound cholesterol molecules were observed for NTS1p, resembling crystal-packing contacts between β_2-adrenergic receptors (illustrated in Figure 5D).[93]

Since the dimerization patterns of the receptors in NTS1p conformation with and without palmitate were rather similar, mainly the palmitoylation-induced conformational changes of NTS1 resulted in adapted dimerization patterns, revealing modified TM1 and H8 interactions. The palmitate anchor showed elevated interactions with cholesterol, and dimers with palmitoyl-recruited cholesterol molecules between interacting monomers could be sampled in the simulation ensemble. In case of the μ-opioid receptor, inhibition of palmitoylation at the intracellular side of TM3 or removal of cholesterol were shown to reduce receptor dimerization and interactions with Gα, indicating a complex interplay between the lipid-guided dimerization and activity of GPCRs.[15,94] Our multiscale simulations suggest dynamic palmitoylation-induced adjustments of receptor conformation, dimerization patterns, and protein−lipid interactions, supporting the hypothesis that lipidation-induced alterations of GPCR function may also occur through modulations of membrane-mediated receptor dimerization.

CONCLUSIONS

In an attempt to characterize the vast influence of the membrane environment on GPCR dimerization and function, we investigated extensive coarse-grained simulation ensembles on the association of NTS1 receptors in various lipid bilayers. Due to the observed overestimation of protein aggregation in the Martini force field[95] a pitfall of our applied simulation strategy could be the sampling of artificial dimer configurations. However, as described in previous studies,[50,51,71,96−98] the combination of coarse-grained models and ensembles of simulations offering ample statistics allows to distinguish between significant and unspecific protein−protein interactions. In the present study, main NTS1 dimer interfaces obtained from coarse-grained simulations are in strong agreement with experimentally observed dimer complexes.[59]

We demonstrate several, distinct protein−lipid interaction profiles altering protein−protein interaction fingerprints. Thereby, general membrane properties, the presence of specific membrane components, and protein−lipidation were identified to steer GPCR dimerization. Lipid tail length and saturation were revealed to exert strong influence on dimerization patterns. Increased fatty acid chain lengths of mainly saturated lipids elevated the hydrophobic mismatch with NTS1 resulting in rapid, rather unspecific receptor association profiles. In turn, higher degrees of unsaturation in fatty acids caused a drastically reduced formation of compact receptor dimers due to facilitated lipid adhesion at the receptor surface. The latter observation supports the hypothesis of a lipid-entropy-driven transmembrane protein association conceptually similar to the hydrophobic effect guiding solute aggregation in water.[92] Binding spots for specific lipid types on the protein surface were further revealed to guide receptor dimerization. Accumulation of cholesterol molecules at TM5,6 NTS1 segments resulted in the formation of a cholesterol wedge at the symmetric TM5,6/TM5,6 interface leading to loosely packed dimer interfaces. Furthermore, binding of anionic lipids mainly to the positively charged intracellular part on TM4 allowed the formation of symmetric TM3,4 dimers where anionic lipids completely pervade the intracellular interaction interface between receptors demonstrating the role of lipids as active parts within transmembrane protein complexes. Thereby, different dimer interfaces may exert distinct receptor activity profiles, allowing the membrane environment to regulate the cellular response to extracellular signals. Due to the high number of possible dimer interfaces, complexes including more than two monomers could be imagined, however, FRET studies on NTS1 indicated predominantly dimers instead of higher-order oligomers.[58,59]

The dimerization of class A GPCRs remains a subject of intense research striving to fully characterize the highly allosteric nature of receptor signaling. Our study provides strong evidence that particular care should be taken considering the membrane environment in experiments addressing GPCR dimerization. Conflicting reports regarding GPCR dimerization may partly result from different experimental membrane environments. In case of NTS1, we could confirm experimentally suggested dimer interfaces especially for bilayer compositions mimicking the experimental setup, illuminating the potential of MD simulations to provide molecular insight into mechanisms behind lipid-guided receptor interactions and highlighting the striking role of the lipid environment in GPCR dimerization.

ASSOCIATED CONTENT

Supporting Information

The Supporting Information is available free of charge at https://pubs.acs.org/doi/10.1021/acs.jpcb.0c00062.

Additional information on main dimer interfaces (center-of-mass distances between interacting monomers, first contact dimer interfaces), estimated hydrophobic mismatch for all used membrane models, models of dimers coupled to G proteins, and detailed descriptions of applied methods (PDF)

https://dx.doi.org/10.1021/acs.jpcb.0c00062
J. Phys. Chem. B 2020, 124, 2823−2834

AUTHOR INFORMATION

Corresponding Authors

Stefan Gahbauer − *Computational Biology, Friedrich-Alexander-University Erlangen-Nüremberg, Erlangen, Germany*; Email: stefan.gahbauer@fau.de

Rainer A. Böckmann − *Computational Biology, Friedrich-Alexander-University Erlangen-Nüremberg, Erlangen, Germany*; Phone: +49 9131 85 25409; Email: rainer.boeckmann@fau.de

Complete contact information is available at: https://pubs.acs.org/10.1021/acs.jpcb.0c00062

Notes

The authors declare no competing financial interest.

ACKNOWLEDGMENTS

This work was supported by the German Science Foundation (DFG) within the Research Training Group 1962, Dynamic Interactions at Biological Membranes, and the SFB1027, Physical Modeling of Non-Equilibrium Processes in Biological Systems. Computer time was provided by the Computing Center of the University Erlangen-Nürnberg (RRZE). We thank Kristyna Pluhackova for support in deriving the lipid force field parameters. We thank Anthony Watts and Steven Lavington for insightful discussions and hosting S.G. at the Department of Biochemistry at Oxford University.

REFERENCES

(1) Hilger, D.; Masureel, M.; Kobilka, B. K. Structure and dynamics of GPCR signaling complexes. *Nat. Struct. Mol. Biol.* **2018**, *25*, 4−12.

(2) Hauser, A. S.; Attwood, M. M.; Rask-Andersen, M.; Schiöth, H. B.; Gloriam, D. E. Trends in GPCR drug discovery: new agents, targets and indications. *Nat. Rev. Drug Discovery* **2017**, *16*, 829−842.

(3) Roth, B. L.; Irwin, J. J.; Shoichet, B. K. Discovery of new GPCR ligands to illuminate new biology. *Nat. Chem. Biol.* **2017**, *13*, 1143−1151.

(4) Sezgin, E.; Levental, I.; Mayor, S.; Eggeling, C. The mystery of membrane organization: composition, regulation and roles of lipid rafts. *Nat. Rev. Mol. Cell Biol.* **2017**, *18*, 361−374.

(5) Harayama, T.; Riezman, H. Understanding the diversity of membrane lipid composition. *Nat. Rev. Mol. Cell Biol.* **2018**, *19*, 281−296.

(6) Ostrom, R. S.; Insel, P. A. The evolving role of lipid rafts and caveolae in G protein-coupled receptor signaling: implications for molecular pharmacology. *Br. J. Pharmacol.* **2004**, *143*, 235−245.

(7) Alves, I. D.; Salamon, Z.; Hruby, V. J.; Tollin, G. Ligand modulation of lateral segregation of a G-protein-coupled receptor into lipid microdomains in sphingomyelin/phosphatidylcholine solid-supported bilayers. *Biochemistry* **2005**, *44*, 9168−9178.

(8) Villar, V. A. M.; Cuevas, S.; Zheng, X.; Jose, P. A. Localization and signaling of GPCRs in lipid rafts. *Methods Cell Biol.* **2016**, *132*, 3−23.

(9) Gahbauer, S.; Böckmann, R. A. Membrane-mediated oligomerization of G protein coupled receptors and its implications for GPCR function. *Front. Physiol.* **2016**, *7*, 00494.

(10) Dawaliby, R.; Trubbia, C.; Delporte, C.; Masureel, M.; Van Antwerpen, P.; Kobilka, B. K.; Govaerts, C. Allosteric regulation of G protein−coupled receptor activity by phospholipids. *Nat. Chem. Biol.* **2016**, *12*, 35−39.

(11) Gutierrez, M. G.; Deyell, J.; White, K. L.; Dalle Ore, L. C.; Cherezov, V.; Stevens, R. C.; Malmstadt, N. The lipid phase preference of the adenosine A 2A receptor depends on its ligand binding state. *Chem. Commun.* **2019**, *55*, 5724−5727.

(12) Strohman, M. J.; Maeda, S.; Hilger, D.; Masureel, M.; Du, Y.; Kobilka, B. K. Local membrane charge regulates β 2 adrenergic receptor coupling to Gi3. *Nat. Commun.* **2019**, *10*, 2234.

(13) Qanbar, R.; Bouvier, M. Role of palmitoylation/depalmitoylation reactions in G-protein-coupled receptor function. *Pharmacol. Ther.* **2003**, *97*, 1−33.

(14) Petäjä-Repo, U. E.; Hogue, M.; Leskelä, T. T.; Markkanen, P. M.; Tuusa, J. T.; Bouvier, M. Distinct subcellular localization for constitutive and agonist-modulated palmitoylation of the human δ opioid receptor. *J. Biol. Chem.* **2006**, *281*, 15780−15789.

(15) Zheng, H.; Pearsall, E. A.; Hurst, D. P.; Zhang, Y.; Chu, J.; Zhou, Y.; Reggio, P. H.; Loh, H. H.; Law, P.-Y. Palmitoylation and membrane cholesterol stabilize μ-opioid receptor homodimerization and G protein coupling. *BMC Cell Biol.* **2012**, *13*, 6.

(16) Lorent, J. H.; Diaz-Rohrer, B.; Lin, X.; Spring, K.; Gorfe, A. A.; Levental, K. R.; Levental, I. Structural determinants and functional consequences of protein affinity for membrane rafts. *Nat. Commun.* **2017**, *8*, 1219.

(17) Naumenko, V. S.; Ponimaskin, E. Palmitoylation as a functional regulator of neurotransmitter receptors. *Neural Plast.* **2018**, *2018*, 1.

(18) Bouvier, M. Oligomerization of G-protein-coupled transmitter receptors. *Nat. Rev. Neurosci.* **2001**, *2*, 274−286.

(19) Urizar, E.; Yano, H.; Kolster, R.; Galés, C.; Lambert, N.; Javitch, J. A. CODA-RET reveals functional selectivity as a result of GPCR heteromerization. *Nat. Chem. Biol.* **2011**, *7*, 624−630.

(20) Bouvier, M.; Hébert, T. E. CrossTalk proposal: weighing the evidence for Class A GPCR dimers, the evidence favours dimers. *J. Physiol.* **2014**, *592*, 2439−2441.

(21) Armando, S.; Quoyer, J.; Lukashova, V.; Maiga, A.; Percherancier, Y.; Heveker, N.; Pin, J.-P.; Prézeau, L.; Bouvier, M. The chemokine CXC4 and CC2 receptors form homo-and heterooligomers that can engage their signaling G-protein effectors and βarrestin. *FASEB J.* **2014**, *28*, 4509−4523.

(22) Wang, W.; Qiao, Y.; Li, Z. New insights into modes of GPCR activation. *Trends Pharmacol. Sci.* **2018**, *39*, 367−386.

(23) Pin, J.-P.; Kniazeff, J.; Prézeau, L.; Liu, J.-F.; Rondard, P. GPCR interaction as a possible way for allosteric control between receptors. *Mol. Cell. Endocrinol.* **2019**, *486*, 89−95.

(24) Felce, J. H.; MacRae, A.; Davis, S. J. Constraints on GPCR heterodimerization revealed by the type-4 induced-association BRET assay. *Biophys. J.* **2019**, *116*, 31−41.

(25) Calebiro, D.; Rieken, F.; Wagner, J.; Sungkaworn, T.; Zabel, U.; Borzi, A.; Cocucci, E.; Zürn, A.; Lohse, M. J. Single-molecule analysis of fluorescently labeled G-protein−coupled receptors reveals complexes with distinct dynamics and organization. *Proc. Natl. Acad. Sci. U. S. A.* **2013**, *110*, 743−748.

(26) Kasai, R. S.; Kusumi, A. Single-molecule imaging revealed dynamic GPCR dimerization. *Curr. Opin. Cell Biol.* **2014**, *27*, 78−86.

(27) Kasai, R. S.; Ito, S. V.; Awane, R. M.; Fujiwara, T. K.; Kusumi, A. The class-A GPCR dopamine D2 receptor forms transient dimers stabilized by agonists: detection by single-molecule tracking. *Cell Biochem. Biophys.* **2018**, *76*, 29−37.

(28) Guo, W.; Urizar, E.; Kralikova, M.; Mobarec, J. C.; Shi, L.; Filizola, M.; Javitch, J. A. Dopamine D2 receptors form higher order oligomers at physiological expression levels. *EMBO J.* **2008**, *27*, 2293−2304.

(29) Manglik, A.; Kruse, A. C.; Kobilka, T. S.; Thian, F. S.; Mathiesen, J. M.; Sunahara, R. K.; Pardo, L.; Weis, W. I.; Kobilka, B. K.; Granier, S. Crystal structure of the μ-opioid receptor bound to a morphinan antagonist. *Nature* **2012**, *485*, 321−326.

(30) Xue, L.; Rovira, X.; Scholler, P.; Zhao, H.; Liu, J.; Pin, J.-P.; Rondard, P. Major ligand-induced rearrangement of the heptahelical domain interface in a GPCR dimer. *Nat. Chem. Biol.* **2015**, *11*, 134−140.

(31) Cordomí, A.; Navarro, G.; Aymerich, M. S.; Franco, R. Structures for G-protein-coupled receptor tetramers in complex with G proteins. *Trends Biochem. Sci.* **2015**, *40*, 548−551.

(32) Felce, J. H.; Latty, S. L.; Knox, R. G.; Mattick, S. R.; Lui, Y.; Lee, S. F.; Klenerman, D.; Davis, S. J. Receptor quaternary organization explains G protein-coupled receptor family structure. *Cell Rep.* **2017**, *20*, 2654−2665.

(33) Borroto-Escuela, D. O.; Rodriguez, D.; Romero-Fernandez, W.; Kapla, J.; Jaiteh, M.; Ranganathan, A.; Lazarova, T.; Fuxe, K.; Carlsson, J. Mapping the interface of a GPCR dimer: a structural model of the A2A adenosine and D2 dopamine receptor heteromer. *Front. Pharmacol.* **2018**, *9*, 00829.
(34) Gupta, K.; Donlan, J. A.; Hopper, J. T.; Uzdavinys, P.; Landreh, M.; Struwe, W. B.; Drew, D.; Baldwin, A. J.; Stansfeld, P. J.; Robinson, C. V. The role of interfacial lipids in stabilizing membrane protein oligomers. *Nature* **2017**, *541*, 421−424.
(35) Periole, X. Interplay of G protein-coupled receptors with the membrane: insights from supra-atomic coarse grain molecular dynamics simulations. *Chem. Rev.* **2017**, *117*, 156−185.
(36) Marrink, S. J.; Corradi, V.; Souza, P. C.; Ingólfsson, H. I.; Tieleman, D. P.; Sansom, M. S. Computational modeling of realistic cell membranes. *Chem. Rev.* **2019**, *119*, 6184−6226.
(37) Muller, M. P.; Jiang, T.; Sun, C.; Lihan, M.; Pant, S.; Mahinthichaichan, P.; Trifan, A.; Tajkhorshid, E. Characterization of lipid-protein interactions and lipid-mediated modulation of membrane protein function through molecular simulation. *Chem. Rev.* **2019**, *119*, 6086−6161.
(38) Manna, M.; Niemelä, M.; Tynkkynen, J.; Javanainen, M.; Kulig, W.; Müller, D. J.; Rog, T.; Vattulainen, I. Mechanism of allosteric regulation of β2-adrenergic receptor by cholesterol. *eLife* **2016**, *5*, No. e18432.
(39) Prasanna, X.; Sengupta, D.; Chattopadhyay, A. Cholesterol-dependent conformational plasticity in GPCR dimers. *Sci. Rep.* **2016**, *6*, 31858.
(40) Guixà-González, R.; Albasanz, J. L.; Rodriguez-Espigares, I.; Pastor, M.; Sanz, F.; Martí-Solano, M.; Manna, M.; Martinez-Seara, H.; Hildebrand, P. W.; Martín, M.; et al. Membrane cholesterol access into a G-protein-coupled receptor. *Nat. Commun.* **2017**, *8*, 14505.
(41) Yen, H.-Y.; Hoi, K. K.; Liko, I.; Hedger, G.; Horrell, M. R.; Song, W.; Wu, D.; Heine, P.; Warne, T.; Lee, Y.; et al. PtdIns(4, 5)P2 stabilizes active states of GPCRs and enhances selectivity of G-protein coupling. *Nature* **2018**, *559*, 423−427.
(42) Corradi, V.; Mendez-Villuendas, E.; Ingólfsson, H. I.; Gu, R.-X.; Siuda, I.; Melo, M. N.; Moussatova, A.; DeGagné, L. J.; Sejdiu, B. I.; Singh, G.; et al. Lipid−protein interactions are unique fingerprints for membrane proteins. *ACS Cent. Sci.* **2018**, *4*, 709−717.
(43) Song, W.; Yen, H.-Y.; Robinson, C. V.; Sansom, M. S. State-dependent lipid interactions with the A2a receptor revealed by MD simulations using in vivo-mimetic membranes. *Structure* **2019**, *27*, 392−403.
(44) Mondal, S.; Johnston, J. M.; Wang, H.; Khelashvili, G.; Filizola, M.; Weinstein, H. Membrane driven spatial organization of GPCRs. *Sci. Rep.* **2013**, *3*, 2909.
(45) Guixà-González, R.; Javanainen, M.; Gómez-Soler, M.; Cordobilla, B.; Domingo, J. C.; Sanz, F.; Pastor, M.; Ciruela, F.; Martinez-Seara, H.; Selent, J. Membrane omega-3 fatty acids modulate the oligomerisation kinetics of adenosine A 2A and dopamine D 2 receptors. *Sci. Rep.* **2016**, *6*, 19839.
(46) Marino, K. A.; Prada-Gracia, D.; Provasi, D.; Filizola, M. Impact of lipid composition and receptor conformation on the spatio-temporal organization of μ-opioid receptors in a multi-component plasma membrane model. *PLoS Comput. Biol.* **2016**, *12*, No. e1005240.
(47) Meral, D.; Provasi, D.; Prada-Gracia, D.; Möller, J.; Marino, K.; Lohse, M. J.; Filizola, M. Molecular details of dimerization kinetics reveal negligible populations of transient μ-opioid receptor homodimers at physiological concentrations. *Sci. Rep.* **2018**, *8*, 7705.
(48) Periole, X.; Knepp, A. M.; Sakmar, T. P.; Marrink, S. J.; Huber, T. Structural determinants of the supramolecular organization of G protein-coupled receptors in bilayers. *J. Am. Chem. Soc.* **2012**, *134*, 10959−10965.
(49) Johnston, J. M.; Wang, H.; Provasi, D.; Filizola, M. Assessing the relative stability of dimer interfaces in G protein-coupled receptors. *PLoS Comput. Biol.* **2012**, *8*, No. e1002649.
(50) Pluhackova, K.; Gahbauer, S.; Kranz, F.; Wassenaar, T. A.; Böckmann, R. A. Dynamic cholesterol-conditioned dimerization of the G protein coupled chemokine receptor type 4. *PLoS Comput. Biol.* **2016**, *12*, No. e1005169.
(51) Gahbauer, S.; Pluhackova, K.; Böckmann, R. A. Closely related, yet unique: Distinct homo-and heterodimerization patterns of G protein coupled chemokine receptors and their fine-tuning by cholesterol. *PLoS Comput. Biol.* **2018**, *14*, No. e1006062.
(52) Mustain, W. C.; Rychahou, P. G.; Evers, B. M. The role of neurotensin in physiologic and pathologic processes. *Curr. Opin. Endocrinol., Diabetes Obes.* **2011**, *18*, 75−82.
(53) White, J. F.; Noinaj, N.; Shibata, Y.; Love, J.; Kloss, B.; Xu, F.; Gvozdenovic-Jeremic, J.; Shah, P.; Shiloach, J.; Tate, C. G.; et al. Structure of the agonist-bound neurotensin receptor. *Nature* **2012**, *490*, 508−513.
(54) Kleczkowska, P.; Lipkowski, A. W. Neurotensin and neurotensin receptors: characteristic, structure−activity relationship and pain modulationa review. *Eur. J. Pharmacol.* **2013**, *716*, 54−60.
(55) Li, J.; Song, J.; Zaytseva, Y. Y.; Liu, Y.; Rychahou, P.; Jiang, K.; Starr, M. E.; Kim, J. T.; Harris, J. W.; Yiannikouris, F. B.; et al. An obligatory role for neurotensin in high-fat-diet-induced obesity. *Nature* **2016**, *533*, 411−415.
(56) White, J. F.; Grodnitzky, J.; Louis, J. M.; Trinh, L. B.; Shiloach, J.; Gutierrez, J.; Northup, J. K.; Grisshammer, R. Dimerization of the class A G protein-coupled neurotensin receptor NTS1 alters G protein interaction. *Proc. Natl. Acad. Sci. U. S. A.* **2007**, *104*, 12199−12204.
(57) Casciari, D.; Dell'Orco, D.; Fanelli, F. Homodimerization of neurotensin 1 receptor involves helices 1, 2, and 4: insights from quaternary structure predictions and dimerization free energy estimations. *J. Chem. Inf. Model.* **2008**, *48*, 1669−1678.
(58) Harding, P. J.; Attrill, H.; Boehringer, J.; Ross, S.; Wadhams, G. H.; Smith, E.; Armitage, J. P.; Watts, A. Constitutive dimerization of the G-protein coupled receptor, neurotensin receptor 1, reconstituted into phospholipid bilayers. *Biophys. J.* **2009**, *96*, 964−973.
(59) Dijkman, P. M.; Castell, O. K.; Goddard, A. D.; Munoz-Garcia, J. C.; De Graaf, C.; Wallace, M. I.; Watts, A. Dynamic tuneable G protein-coupled receptor monomer-dimer populations. *Nat. Commun.* **2018**, *9*, 1710.
(60) Dathe, A.; Heitkamp, T.; Pérez, I.; Sielaff, H.; Westphal, A.; Reuter, S.; Mrowka, R.; Börsch, M. Observing monomer: dimer transitions of neurotensin receptors 1 in single SMALPs by homoFRET and in an ABELtrap. *Single Molecule Spectroscopy and Superresolution Imaging XII* **2019**, 8.
(61) Börsch, M.; Westphal, A.; Sielaff, H.; Reuter, S.; Heitkamp, T.; Mrowka, R. Ligand-induced oligomerization of the human GPCR neurotensin receptor 1 monitored in living HEK293T cells. *Multi-photon Microscopy in the Biomedical Sciences XIX* **2019**, 31.
(62) Oates, J.; Faust, B.; Attrill, H.; Harding, P.; Orwick, M.; Watts, A. The role of cholesterol on the activity and stability of neurotensin receptor 1. *Biochim. Biophys. Acta, Biomembr.* **2012**, *1818*, 2228−2233.
(63) Inagaki, S.; Ghirlando, R.; White, J. F.; Gvozdenovic-Jeremic, J.; Northup, J. K.; Grisshammer, R. Modulation of the interaction between neurotensin receptor NTS1 and Gq protein by lipid. *J. Mol. Biol.* **2012**, *417*, 95−111.
(64) Dijkman, P. M.; Watts, A. Lipid modulation of early G protein-coupled receptor signalling events. *Biochim. Biophys. Acta, Biomembr.* **2015**, *1848*, 2889−2897.
(65) Bolivar, J. H.; Munoz-Garcia, J. C.; Castro-Dopico, T.; Dijkman, P. M.; Stansfeld, P. J.; Watts, A. Interaction of lipids with the neurotensin receptor 1. *Biochim. Biophys. Acta, Biomembr.* **2016**, *1858*, 1278−1287.
(66) Heakal, Y.; Woll, M. P.; Fox, T.; Seaton, K.; Levenson, R.; Kester, M. Neurotensin receptor-1 inducible palmitoylation is required for efficient receptor-mediated mitogenic-signaling within structured membrane microdomains. *Cancer Biol. Ther.* **2011**, *12*, 427−435.
(67) Krumm, B. E.; White, J. F.; Shah, P.; Grisshammer, R. Structural prerequisites for G-protein activation by the neurotensin receptor. *Nat. Commun.* **2015**, *6*, 7895.
(68) Berman, H. M.; Westbrook, J.; Feng, Z.; Gilliland, G.; Bhat, T. N.; Weissig, H.; Shindyalov, I. N.; Bourne, P. E. The protein data bank. *Nucleic Acids Res.* **2000**, *28*, 235−242.

https://dx.doi.org/10.1021/acs.jpcb.0c00062
J. Phys. Chem. B 2020, 124, 2823−2834

(69) Egloff, P.; Hillenbrand, M.; Klenk, C.; Batyuk, A.; Heine, P.; Balada, S.; Schlinkmann, K. M.; Scott, D. J.; Schütz, M.; Plückthun, A. Structure of signaling-competent neurotensin receptor 1 obtained by directed evolution in Escherichia coli. *Proc. Natl. Acad. Sci. U. S. A.* **2014**, *111*, E655−E662.
(70) Huang, J.; Lakkaraju, S. K.; Coop, A.; MacKerell, A. D., Jr Conformational heterogeneity of intracellular loop 3 of the μ-opioid G-protein coupled receptor. *J. Phys. Chem. B* **2016**, *120*, 11897−11904.
(71) Wassenaar, T. A.; Pluhackova, K.; Moussatova, A.; Sengupta, D.; Marrink, S. J.; Tieleman, D. P.; Böckmann, R. A. High-throughput simulations of dimer and trimer assembly of membrane proteins. The DAFT approach. *J. Chem. Theory Comput.* **2015**, *11*, 2278−2291.
(72) de Jong, D. H.; Singh, G.; Bennett, W. D.; Arnarez, C.; Wassenaar, T. A.; Schäfer, L. V.; Periole, X.; Tieleman, D. P.; Marrink, S. J. Improved parameters for the martini coarse-grained protein force field. *J. Chem. Theory Comput.* **2013**, *9*, 687−697.
(73) Pronk, S.; Páll, S.; Schulz, R.; Larsson, P.; Bjelkmar, P.; Apostolov, R.; Shirts, M. R.; Smith, J. C.; Kasson, P. M.; Van Der Spoel, D.; et al. GROMACS 4.5: a high-throughput and highly parallel open source molecular simulation toolkit. *Bioinformatics* **2013**, *29*, 845−854.
(74) Wassenaar, T. A.; Pluhackova, K.; Böckmann, R. A.; Marrink, S. J.; Tieleman, D. P. Going backward: a flexible geometric approach to reverse transformation from coarse grained to atomistic models. *J. Chem. Theory Comput.* **2014**, *10*, 676−690.
(75) Huang, J.; Rauscher, S.; Nawrocki, G.; Ran, T.; Feig, M.; de Groot, B. L.; Grubmüller, H.; MacKerell, A. D., Jr CHARMM36m: an improved force field for folded and intrinsically disordered proteins. *Nat. Methods* **2017**, *14*, 71−73.
(76) Abraham, M. J.; Murtola, T.; Schulz, R.; Páll, S.; Smith, J. C.; Hess, B.; Lindahl, E. GROMACS: high performance molecular simulations through multi-level parallelism from laptops to supercomputers. *SoftwareX* **2015**, *1*, 19−25.
(77) Breckenridge, W.; Morgan, I.; Zanetta, J.; Vincendon, G. Adult rat brain synaptic vesicles II. Lipid composition. *Biochim. Biophys. Acta, Gen. Subj.* **1973**, *320*, 681−686.
(78) Martínez, M.; Mougan, I. Fatty acid composition of human brain phospholipids during normal development. *J. Neurochem.* **1998**, *71*, 2528−2533.
(79) Wassenaar, T. A.; Ingólfsson, H. I.; Böckmann, R. A.; Tieleman, D. P.; Marrink, S. J. Computational lipidomics with insane: a versatile tool for generating custom membranes for molecular simulations. *J. Chem. Theory Comput.* **2015**, *11*, 2144−2155.
(80) Rasmussen, S. G.; DeVree, B. T.; Zou, Y.; Kruse, A. C.; Chung, K. Y.; Kobilka, T. S.; Thian, F. S.; Chae, P. S.; Pardon, E.; Calinski, D.; et al. Crystal structure of the β 2 adrenergic receptor−Gs protein complex. *Nature* **2011**, *477*, 549−555.
(81) Thal, D. M.; Glukhova, A.; Sexton, P. M.; Christopoulos, A. Structural insights into G-protein-coupled receptor allostery. *Nature* **2018**, *559*, 45−55.
(82) Weis, W. I.; Kobilka, B. K. The molecular basis of G protein-coupled receptor activation. *Annu. Rev. Biochem.* **2018**, *87*, 897−919.
(83) Warne, T.; Edwards, P. C.; Doré, A. S.; Leslie, A. G.; Tate, C. G. Molecular basis for high-affinity agonist binding in GPCRs. *Science* **2019**, *364*, 775−778.
(84) Capper, M. J.; Wacker, D. How the ubiquitous GPCR receptor family selectively activates signalling pathways. *Nature* **2018**, *558*, 529−530.
(85) Kato, H. E.; Zhang, Y.; Hu, H.; Suomivuori, C.-M.; Kadji, F. M. N.; Aoki, J.; Krishna Kumar, K.; Fonseca, R.; Hilger, D.; Huang, W.; et al. Conformational transitions of a neurotensin receptor 1−G i1 complex. *Nature* **2019**, *572*, 80−85.
(86) Besserer-Offroy, É.; Brouillette, R. L.; Lavenus, S.; Froehlich, U.; Brumwell, A.; Murza, A.; Longpré, J.-M.; Marsault, É.; Grandbois, M.; Sarret, P.; et al. The signaling signature of the neurotensin type 1 receptor with endogenous ligands. *Eur. J. Pharmacol.* **2017**, *805*, 1−13.
(87) Javanainen, M.; Enkavi, G.; Guixà-Gonzaléz, R.; Kulig, W.; Martinez-Seara, H.; Levental, I.; Vattulainen, I. Reduced level of docosahexaenoic acid shifts GPCR neuroreceptors to less ordered membrane regions. *PLoS Comput. Biol.* **2019**, *15*, No. e1007033.
(88) Feller, S. E.; Gawrisch, K.; Woolf, T. B. Rhodopsin exhibits a preference for solvation by polyunsaturated docosohexaenoic acid. *J. Am. Chem. Soc.* **2003**, *125*, 4434−4435.
(89) Pitman, M. C.; Grossfield, A.; Suits, F.; Feller, S. E. Role of cholesterol and polyunsaturated chains in lipid- protein interactions: molecular dynamics simulation of rhodopsin in a realistic membrane environment. *J. Am. Chem. Soc.* **2005**, *127*, 4576−4577.
(90) Grossfield, A.; Feller, S. E.; Pitman, M. C. Contribution of omega-3 fatty acids to the thermodynamics of membrane protein solvation. *J. Phys. Chem. B* **2006**, *110*, 8907−8909.
(91) Sabra, M. C.; Uitdehaag, J. C.; Watts, A. General model for lipid-mediated two-dimensional array formation of membrane proteins: application to bacteriorhodopsin. *Biophys. J.* **1998**, *75*, 1180−1188.
(92) Helms, V. Attraction within the membrane: forces behind transmembrane protein folding and supramolecular complex assembly. *EMBO Rep.* **2002**, *3*, 1133−1138.
(93) Cherezov, V.; Rosenbaum, D. M.; Hanson, M. A.; Rasmussen, S. G.; Thian, F. S.; Kobilka, T. S.; Choi, H.-J.; Kuhn, P.; Weis, W. I.; Kobilka, B. K.; et al. High-resolution crystal structure of an engineered human β2-adrenergic G protein-coupled receptor. *Science* **2007**, *318*, 1258−1265.
(94) Goddard, A. D.; Watts, A. Regulation of G protein-coupled receptors by palmitoylation and cholesterol. *BMC Biol.* **2012**, *10*, 27.
(95) Javanainen, M.; Martinez-Seara, H.; Vattulainen, I. Excessive aggregation of membrane proteins in the Martini model. *PLoS One* **2017**, *12*, e0187936.
(96) Han, J.; Pluhackova, K.; Wassenaar, T. A.; Böckmann, R. A. Synaptobrevin transmembrane domain dimerization studied by multiscale molecular dynamics simulations. *Biophys. J.* **2015**, *109*, 760−771.
(97) Larisch, N.; Kirsch, S.; Schambony, A.; Studtrucker, T.; Böckmann, R. A.; Dietrich, P. The function of the two-pore channel TPC1 depends on dimerization of its carboxy-terminal helix. *Cell. Mol. Life Sci.* **2016**, *73*, 2565−2581.
(98) Han, J.; Pluhackova, K.; Böckmann, R. A. Exploring the formation and the structure of synaptobrevin oligomers in a model membrane. *Biophys. J.* **2016**, *110*, 2004−2015.

https://dx.doi.org/10.1021/acs.jpcb.0c00062
J. Phys. Chem. B 2020, 124, 2823−2834